New Journal of Physics
The open access journal at the forefront of physics

Deutsche Physikalische Gesellschaft DPG IOP Institute of Physics

PAPER • OPEN ACCESS

Importance of the dielectric contrast for the polarization of excitonic transitions in single GaN nanowires

To cite this article: Pierre Corfdir *et al* 2015 *New J. Phys.* **17** 033040

New Journal of Physics
The open access journal at the forefront of physics

Deutsche Physikalische Gesellschaft DPG
IOP Institute of Physics

Published in partnership with: Deutsche Physikalische Gesellschaft and the Institute of Physics

OPEN ACCESS

RECEIVED
21 October 2014

REVISED
28 January 2015

ACCEPTED FOR PUBLICATION
23 February 2015

PUBLISHED
27 March 2015

PAPER

Importance of the dielectric contrast for the polarization of excitonic transitions in single GaN nanowires

Pierre Corfdir, Felix Feix, Johannes K Zettler, Sergio Fernández-Garrido and Oliver Brandt

Paul-Drude-Institut für Festkörperelektronik, Hausvogteiplatz 5-7, D-10117 Berlin, Germany

E-mail: corfdir@pdi-berlin.de

Keywords: GaN nanowires, photoluminescence, exciton, polarization

Abstract

We investigate the polarization of excitonic transitions of single dispersed GaN nanowires with a diameter of about 50 nm. We observe donor-bound exciton transitions with a linewidth narrower than 250 μeV at 10 K, whereas the luminescence from free excitons exhibits a width of up to 5 meV. This broadening is larger than that observed for free excitons in the as-grown nanowire ensemble and is the result of inhomogeneous strain introduced by the nanowire dispersion. This strain lowers the symmetry of the lattice structure and allows A excitons to emit light polarized parallel to the nanowire axis. The polarization anisotropy of A excitons, however, is found to largely vary from one nanowire to another. In addition, the various bound-exciton lines in a given nanowire do not show the same polarization anisotropies. These findings can be explained by the dielectric contrast between the nanowire and its environment, but only when taking into account the strong variations of the dielectric function of GaN at the near band-edge.

1. Introduction

The luminescence of semiconductor nanowires and its polarization is a topic of great current interest. The nanowire geometry together with the contrast between the dielectric constant of the nanowire and its surroundings lead to a polarization anisotropy in absorption and emission [1]. This nanowire antenna effect has been observed for nanowires with a diameter ϕ much smaller as well as on the order of the wavelength λ of the nanowire's luminescence [1–8]. In the former case, the antenna effect can be understood by simple electrostatic considerations [1], whereas it is caused by the coupling of light into the guided modes supported by the nanowire for the latter case [3]. However, the magnitude of the polarization anisotropy is not only given by the ratio ϕ/λ, but also depends on the band structure of the material the nanowire consists of. In bulk semiconducting materials with a zincblende crystal structure, the maxima of the heavy and light-hole valence bands are degenerate. The emission from thin nanowires with a zincblende crystal structure is therefore mostly polarized along the nanowire axis, due to the antenna effect [9, 10]. In contrast, for semiconductors with a wurtzite crystal structure such as for group-III nitrides, the two higher-energy valence bands (A and B) at the center of the Brillouin zone are split by the crystal field. The polarization anisotropy of the near band-edge emission of nanowires with wurtzite structure thus depends on the magnitude of the splitting between the A and B valence bands [9–11]. Since the occupation of the A and B bands depends on temperature, a complete reversal of the polarization anisotropy within a few Kelvin can occur for nanowires with crystal-field and spin–orbit splittings such that the A and B bands are close in energy [11].

The complex interplay between band-structure and dielectric effects as well as the resulting possibility to engineer the polarization of their spontaneous emission has motivated several previous spectroscopic investigations of the optical polarization of spontaneously formed GaN nanowires [4, 6, 12, 13]. These nanowires are synthesized by molecular beam epitaxy, and exhibit a length of typically a few μm and a mean diameter of 50–100 nm [14]. Due to this high aspect ratio, spontaneously formed GaN nanowires are invariably found to be free of any net strain, and in the absence of coalescence, also free of microstrain [15]. Despite this

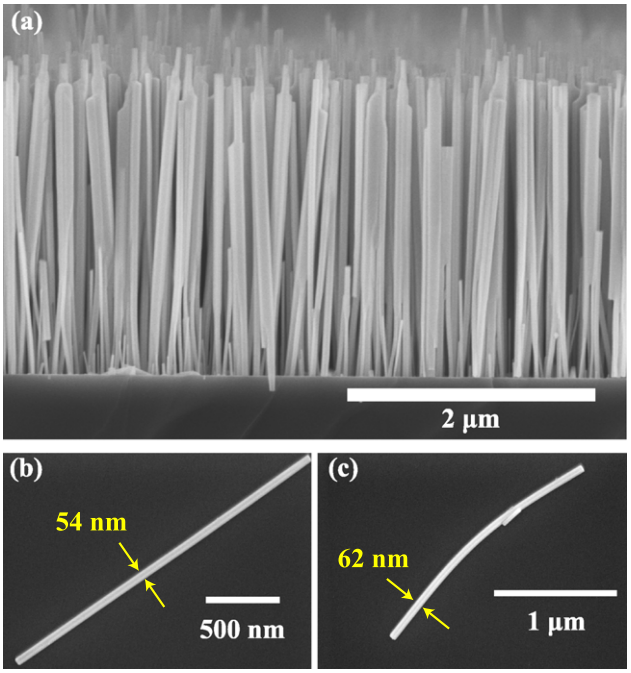

Figure 1. (a) Cross-sectional secondary electron micrograph of the as-grown GaN nanowire ensemble under investigation. (b) and (c) Secondary electron micrographs of two dispersed nanowires. The diameter of each nanowire is indicated in the figure. Note the pronounced bending of the nanowire in (c).

fact, the donor-bound exciton transition dominating their luminescence spectra at 10 K are commonly found to have a width of 1–2 meV [14, 16–18]. This large width partly stems from the surface-induced distortion of the wavefunction of donor-bound excitons [17, 18] and results in a spectral overlap of the transitions involved in the radiative decay of excitons, thus complicating the quantitative analysis of their optical polarization. We have recently reported a significant reduction of the contribution of surface effects to the emission broadening for GaN nanowires grown on Si(111) at a temperature larger than 850 °C [19]. While the morphology of these samples is similar to those observed for nanowires formed at lower temperatures, the donor-bound exciton line in our GaN nanowire ensembles exhibits a linewidth of about 0.5 meV at 10 K [19].

In this work, we study the polarization of the excitonic transitions of single GaN nanowires with an average diameter of 50 nm using polarization-resolved micro-photoluminescence spectroscopy. These nanowires were harvested from a high-temperature grown GaN nanowire ensemble which exhibits sub-meV donor-bound exciton linewidths. For single, dispersed nanowires, we resolve transitions from *single* donor-bound excitons which have a (resolution-limited) linewidth narrower than 250 μeV. The energies of these bound excitons, however, scatter over a few meV, reflecting the presence of strain introduced by the nanowire dispersion. We argue that this strain breaks the wurtzite symmetry of the lattice and mixes the A and B valence bands. This valence-band mixing combined with the antenna effect leads to a different polarization degree for the donor-bound exciton and the corresponding free exciton transition. Moreover, the polarization patterns of the free and bound A excitons are found to be significantly altered with respect to that expected and observed for bulk GaN. In the bulk, the radiative decay of the A exciton is forbidden for light polarized along the *c*-axis of the wurtzite crystal structure, while we observe various (and sometimes essentially isotropic) polarization patterns for single GaN nanowires depending on their actual strain state.

2. Experimental details

The single GaN nanowires studied in this work are taken from a nanowire ensemble which was synthesized by plasma-assisted molecular beam epitaxy on a Si(111) substrate [20–22]. The nanowire axis is parallel to the $[000\bar{1}]$ direction of the wurtzite structure. The nanowires in the as-grown ensemble are on average 2 μm long and exhibit a mean diameter of 50 nm (figure 1(a)). The ensemble was grown at 865 °C using a Ga/N flux ratio higher than one to compensate for the high desorption rate of Ga [23]. The combination of a high substrate temperature and a high Ga flux induces melt-back etching of the Si substrate due to the formation of a Ga–Si eutectic alloy [19]. The melt-back etching of the Si substrate causes an enhanced incorporation of Si in the nanowires as discussed in detail in [19]. This incorporation is inhomogeneous along the nanowire axis. As

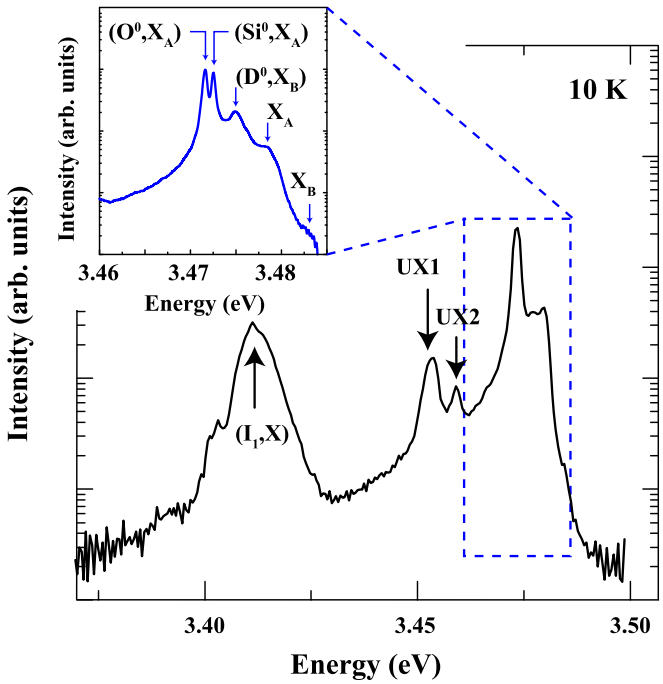

Figure 2. Low-temperature (10 K) photoluminescence spectrum of the GaN nanowire ensemble under investigation. The inset shows a spectrum from the same sample acquired near the band edge with a higher spectral resolution.

shown in [24], cathodoluminescence experiments revealed that the emission from the bottom 1 μm of the nanowires is weak. This finding was attributed to the fact that in the bottom 1 μm part of the nanowires, the Si incorporation is sufficiently large to induce radial electric fields that ionize excitons. For the dispersal of these nanowires, a piece of the as-grown sample was sonicated in isopropanol for 30 min. The solution was then drop-casted using a micropipette on a TiAu mask deposited on a Si substrate. Representative examples of single, dispersed nanowires are displayed in figures 1(b) and (c). The adhesive pinning of the nanowire to the substrate arises from the van der Waals forces and from the contaminant residues of isopropanol and it is strong enough to hold nanowires in states of high bending stress [25].

For photoluminescence spectroscopy, the samples were placed in a cold-finger cryostat facilitating continuous temperature control down to 10 K. For excitation, we used the 325 nm line of a He–Cd laser, attenuated to a power of 1 μW and focused to a 1 μm-diameter spot using a 50× microscope objective with a numerical aperture of 0.65. The photoluminescence of the excited nanowires was collected with the same objective, dispersed by a 80 cm focal length spectrometer equipped with gratings having 600 and 2400 grooves per mm, and detected with a CCD. The spectral resolution of the setup is 0.25 meV with the 2400 grooves per mm grating. Experiments on the nanowire ensemble were carried out with the light wavevector $\mathbf{k}$ parallel to the nanowire axis, whereas for measurements on dispersed nanowires, $\mathbf{k}$ was perpendicular to the nanowire axis, and the electric field $\mathbf{E}$ was in the plane whose normal is parallel to $\mathbf{k}$. The analysis of the polarization of the nanowire emission was carried out with a half-waveplate followed by a polarizer. The polarizer axis is fixed and its orientation is such that the diffraction efficiency of the grating is maximum. The analysis of the emission is obtained by rotating the half waveplate. The angle between the nanowire and the polarization axis of the detected light is denoted as θ.

3. Photoluminescence of ensemble and single GaN nanowires

Figure 2 displays a photoluminescence spectrum at 10 K of the as-grown GaN nanowire ensemble shown in figure 1(a). The spectrum is dominated by transitions from donor-bound and free excitons (dashed rectangle) which will be discussed in detail below. In addition, the spectrum exhibits two bands at 3.4526 and 3.4585 eV, labeled UX_1 and UX_2, respectively, that arise from the recombination of excitons bound to an unknown point defect which is thought to be related to the nanowire surface [13, 14, 17, 26, 27]. The UX_1 and UX_2 bands overlap spectrally with the two-electron satellites of the donor-bound excitons from the core of the nanowires [17], making the analysis of their fine structure complicated. Furthermore, the broad band at about 3.41 eV stems from the recombination of excitons bound to I_1 stacking faults [(I_1, X)]. The enhanced Si incorporation in our GaN nanowires is accompanied by a reduction in the formation energy of these defects [28], leading to a strong

(I_1, X) emission at 10 K [19]. The (I_1, X) emission has been studied in detail in [24] and will not be discussed further.

The inset of figure 2 shows the near-band edge region of the PL spectrum with higher spectral resolution. Here, the donor-bound exciton transition is seen to be composed of two lines centered at 3.4719 and 3.4728 eV that we ascribe to the recombination of A excitons bound to neutral O [(O^0, X_A)] and to neutral Si [(Si^0, X_A)] donors. In agreement with the result of [19], using a growth temperature larger than about 850 °C leads to the melt-back etching of the Si substrate and thus to an enhanced incorporation of Si in the GaN nanowires, as confirmed by the intense (Si^0, X_A) line observed in the spectrum. For this particular sample, the (O^0, X_A) and the (Si^0, X_A) transitions exhibit a full width at half maximum (FWHM) below 600 μeV. This observation is a direct consequence of the incorporation of Si into our nanowires: the larger the density of donors, the larger the magnitude of the electric fields at the surface of the nanowires and the lower the contribution of surface effects to the linewidth of the donor-bound exciton emission [19].

Additional lines are observed on the high-energy side of the (Si^0, X_A) line. We attribute the band at 3.4757 eV to the recombination of B excitons bound to neutral donors [(D^0, X_B)]. We also identify the emission from free A excitons (X_A) and free B excitons (X_B) centered at 3.4785 and 3.4825 eV, respectively. The energy of the X_A transition indicates that the net strain in our as-grown nanowires is essentially zero. We emphasize that the X_A and X_B transitions are significantly broader (2.7 and 3.7 meV, respectively) than the (O^0, X_A) and (Si^0, X_A) lines. A similar observation was made for the free exciton luminescence in thick layers [29] and is partly due to the fact that the free exciton emission broadening is proportional to kT. In addition, the luminescence of free exciton is associated to the radiative decay of polaritons at the bottleneck of the lower branch and at the bottom of the upper branch [30, 31], and appears as a doublet in high-quality bulk material [29, 31]. However, considering that the mean diameter of our GaN nanowires is 50 nm, that the exciton recombination is mostly nonradiative already at 10 K [32], and that there are strong surface electric fields perpendicular to the nanowire axis [19], we would rather expect a broad singlet [33–35], which is indeed what we observe experimentally.

Figure 3 shows temperature-dependent PL spectra for a single nanowire (hereafter referred to as nanowire NW1) originating from the nanowire ensemble studied above and dispersed on a substrate. The spectrum recorded at 10 K exhibits numerous lines between 3.44 and 3.49 eV with a resolution-limited linewidth of 250 μeV. In contrast, the band at 3.477 eV is an order of magnitude broader (2.8 meV). For an unambiguous identification of the transitions which may be shifted by strain introduced by the dispersion as seen in figure 1(c), we examine their evolution as a function of the temperature.

We first focus on the temperature-dependence of the emission in the 3.461–3.490 eV range. The evolution of the relative intensity of these lines between 10 and 45 K identifies the lines in the range between 3.461 and 3.475 eV as being due to the recombination of excitons bound to neutral donors and neutral acceptors, and the broader bands at 3.477 and 3.482 eV to originate from the decay of the free A and B excitons, respectively [36]. Due to the multitude of lines around 3.47 eV, it is not possible to distinguish between the recombination of excitons bound to Si and O. The recombination of a donor-bound exciton is affected not only by the chemical origin of the donor, but also by the local strain state and by the distance between the donor and the surface [37]. Therefore, for dispersed nanowires, the transitions related to A excitons bound to donors are simply denoted as (D^0, X).

Next, we examine the nature of the resolution-limited lines in the range between 3.440 and 3.460 eV. Their intensity quenches together with the donor-bound exciton transitions when the temperature is increased from 10 to 45 K. This quenching is accompanied by the development of the UX_2 band centered at 3.456 eV and with an FWHM of 7.5 meV at 45 K. This observation is analogous to that of Calleja *et al* [14] for a GaN nanowire ensemble. The evolution of the UX_1 and UX_2 bands with temperature strongly resembles that of (D^0, X) and free excitons. While this observation agrees with the assumption that the UX_1 lines arise from the recombination of an exciton bound to a point defect, it suggests that the UX_2 band is associated to a delocalized state. The nature of this delocalized state, however, is unclear at present. Time-resolved measurements of the decay of this band could reveal the dimensionality of the states from which this emission originates, and could thus clarify whether they stem from a planar defect or not [24].

Figure 4 shows the broadening and the energy measured for the X_A transition for nine different dispersed nanowires. For several of these wires, the X_A transition is redshifted and its broadening is similar to or larger than that observed for the as-grown nanowire ensemble. Dispersed nanowires may become homogeneously strained as a result of the mismatch in thermal expansion between the nanowire and the substrate [16, 18, 38], and heterogeneously strained due to the bending of the nanowire during the dispersion process [39–41]. These homogeneous and heterogeneous strains strongly impact the nanowire emission energy. While Schlager *et al* [38] estimate that homogeneous strain can induce energy shifts up to 13 meV at low temperature, Dietrich *et al* [39] have measured bending-induced energy shifts up to 30 meV in ZnO nanowires. In contrast to the

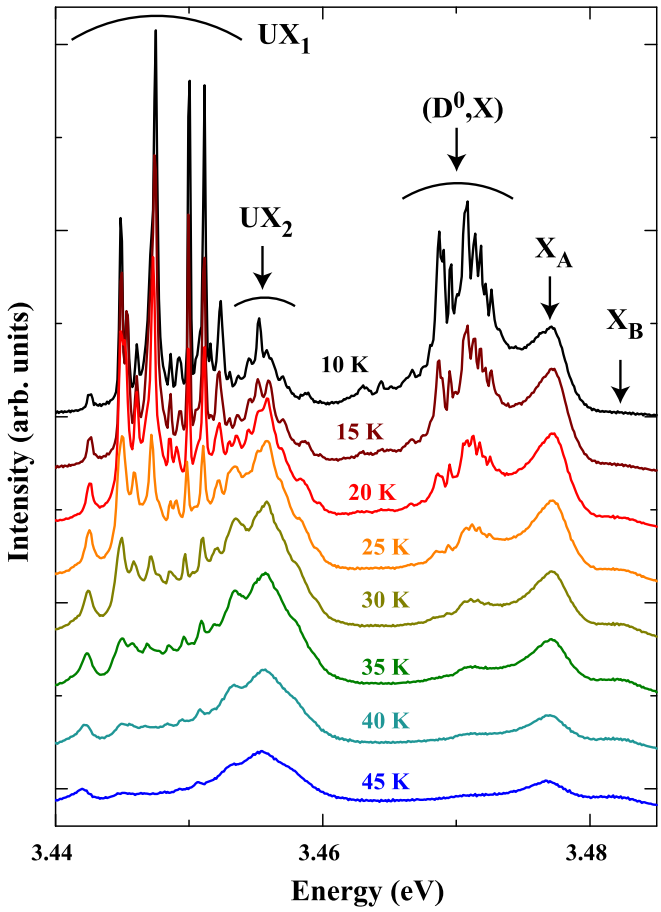

Figure 3. Photoluminescence spectra of nanowire NW1 between 10 and 45 K. The spectra have been shifted vertically for clarity.

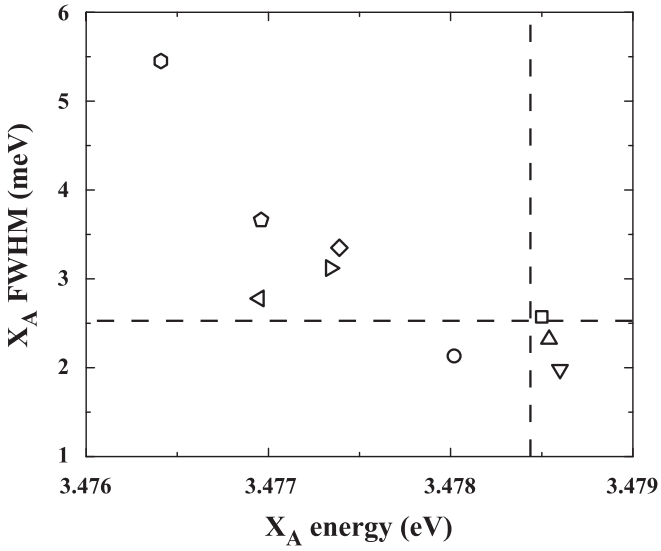

Figure 4. FWHM of the X_A transition at 10 K as a function of its energy for single dispersed GaN nanowires. Each symbol refers to a given nanowire. The FWHM of the X_A transition for nanowires NW1 and NW2 are shown by ◁ and □, respectively. The vertical and horizontal dashed lines show the energy and the FWHM, respectively, of the X_A transition at 10 K for the ensemble of as-grown nanowires.

(D^0, X_A) states, the X_A is delocalized. The broadening of the X_A transition for dispersed wires may therefore provide information on the nature of the strain state in a dispersed nanowire. As discussed in [41], the competition between the recombination and the strain-induced drift of the exciton in the nanowire controls the

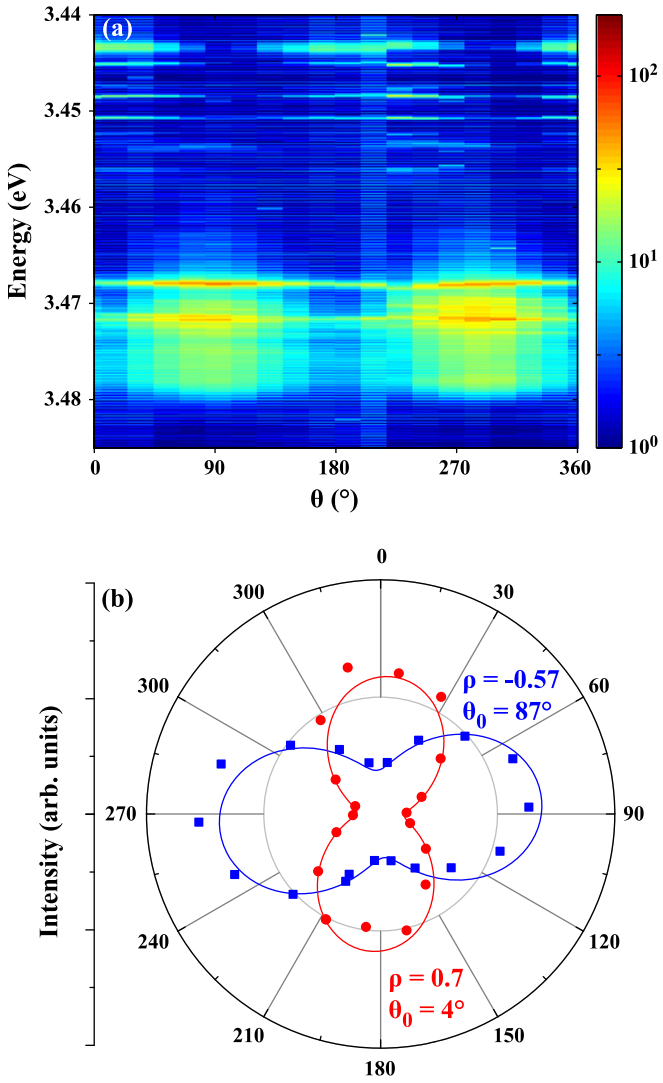

Figure 5. (a) Polarization-resolved photoluminescence map of nanowire NW1 recorded at 10 K. An angle of 0° corresponds to a polarization parallel to the nanowire axis. The intensity is color-coded according to the logarithmic scale displayed in the figure. (b) Polar representation of the nanowire emission intensity integrated between 3.465 and 3.480 eV (squares) and between 3.440 and 3.460 eV (circles). The fits to the experimentally observed angular dependencies of the intensity using equation (1) are shown by solid lines.

peak energy and the broadening of the free exciton PL. We observe for our dispersed nanowires that the emission energy of the X_A is similar to or lower than that observed in the as-grown nanowires (cf figure 2), suggesting that photogenerated excitons drift from compressively to tensilely strained nanowire regions, where they recombine radiatively.

4. Polarization of the excitonic transitions in single GaN nanowires

The difference in experimental geometry for measurements on the ensemble and on dispersed GaN nanowires (see section 2) leads to a strong change in the relative intensities of the UX_1 and (D^0, X_A) lines. For dispersed nanowires, the peak intensity of the UX_1 lines at 10 K is on the same order as that of the (D^0, X) transitions (figure 3), whereas the UX_1 band is about an order of magnitude weaker than the (O^0, X_A) and the (Si^0, X_A) transitions for the nanowire ensemble (figure 2). Sam-Giao *et al* [13] observed the same behavior and interpreted it as being due to the fact that the selection rules for the X_A and for the exciton state involved in the UX_1 transition are different. Figure 5(a) displays the dependence of the PL of nanowire NW1 on the angle θ between the polarizer and the nanowire axis. In agreement with [13], the UX_1 and UX_2 bands are polarized along the nanowire axis, i.e., they are counter-polarized to the (D^0, X_A) and X_A lines. To quantify the emission polarization anisotropy, the θ-dependence of the PL intensity (I) is fit by Malus' law:

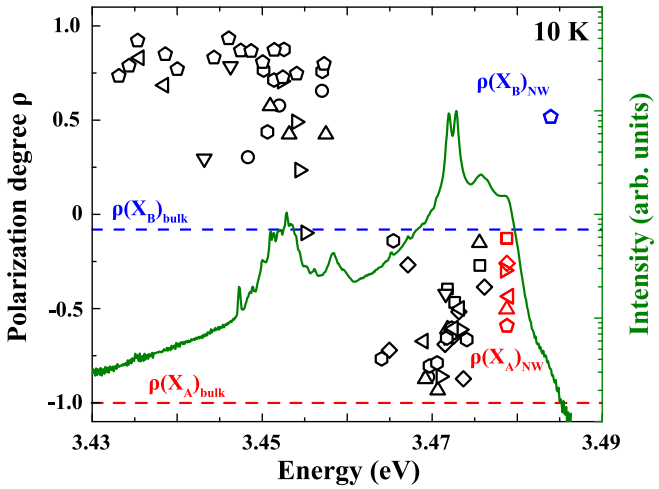

Figure 6. Polarization degree as a function of photoluminescence energy at 10 K for nine dispersed nanowires. Each symbol refers to a given nanowire (nanowires NW1 and NW2 are represented by ◁ and □, respectively). The individual nanowire spectra have been rigidly shifted such that the X_A transition energy in each spectrum matches the one measured for the GaN ensemble. The polarization degrees of the X_A and X_B transitions are displayed by red and blue symbols, respectively. The red and blue dashed lines highlight the polarization degrees measured for the X_A and X_B transitions in strain-free GaN, respectively [42]. The green solid line shows the photoluminescence spectrum of the GaN nanowire ensemble at 10 K.

$$I = I^{\parallel}\cos^2\left(\theta - \theta_0\right) + I^{\perp}\sin^2\left(\theta - \theta_0\right), \tag{1}$$

where $I^{\parallel}$ and $I^{\perp}$ are the emission intensities parallel and perpendicular to the nanowire axis, respectively, and θ_0 is the angle of polarization of the transition. Using equation (1), one can deduce the polarization degree ρ:

$$\rho = \frac{I^{\parallel} - I^{\perp}}{I^{\parallel} + I^{\perp}}. \tag{2}$$

As shown in figure 5(b), the emission integrated between 3.44 and 3.46 eV exhibits a polarization degree ρ of 0.70, while we obtain $\rho = -0.57$ for the emission integrated between 3.465 and 3.480 eV. These values are in good agreement with those of the nanowire ensemble studied by Sam-Giao *et al* [13] who reported values of 0.8 and −0.7 for the UX_1 and (D^0, X_A) transitions, respectively. The values obtained by us as well as in [13] for the (D^0, X_A) deviate markedly from that observed for the bulk and thus also expected for a freestanding GaN nanowire, namely, −1 [42]. This deviation may be caused by a significant contribution of the (D^0, X_B) to the intensity between 3.465 and 3.480 eV, leading to a deviation of its polarization degree from −1. In addition, the use of an objective with a high numerical aperture results in a deviation from $\boldsymbol{k}\perp c$ and may thus lead to the collection of light with a nonzero electric field component along c [6, 29]. Alternatively, the perturbative donor potential may induce a certain degree of mixing between the A and B states. The latter effect would selectively reduce the polarization anisotropy of the (D^0, X_A) compared to that of the X_A.

To clarify this point, we have extracted ρ for each emission line of nanowire NW1. We find that the (D^0, X_A) lines at 3.4673 and 3.4709 eV show values of ρ equal to −0.67 and −0.60, respectively, while we measure $\rho = -0.44$ for the X_A transition. The polarization anisotropy is therefore stronger for the (D^0, X_A) than for the X_A line, at odds with our above speculation on the possible mixing of A and B states by the donor potential. Neither can this observation be explained in terms of relaxation of the $\boldsymbol{k}\perp c$ condition, as the latter deviation cannot yield different values of ρ for the X_A and (D^0, X_A) transitions.

To confirm that our observation does not arise from experimental artifacts, we collected the energy dependence of ρ for several nanowires as shown in figure 6. For clarity, we have shifted each spectrum such that the X_A energy of the dispersed nanowires corresponds to that measured for the nanowire ensemble. As a result, it is straightforward to identify the polarization of the (D^0, X_A), (D^0, X_B), X_A and X_B transitions (cf figure 6). The trends observed corroborate the results obtained on nanowire NW1: the polarization anisotropy of the (D^0, X_A) and X_A transitions is reduced compared to the one for free-standing GaN. For the nine nanowires we have investigated, ρ lies between −0.87 and −0.4 for the (D^0, X_A) and between −0.59 and −0.13 for the X_A transition. Figure 7 shows the photoluminescence spectrum of the nanowire with $\rho = -0.13$ for the X_A line (hereafter denoted as nanowire NW2). The essentially isotropic emission (see inset for the full angular dependence), however, cannot arise from the spectral overlap between the X_A transition and a band polarized parallel to the c axis, since the X_A line of nanowire NW2 is intense and well-separated from the transitions related to the X_B and (D^0, X_B) transitions.

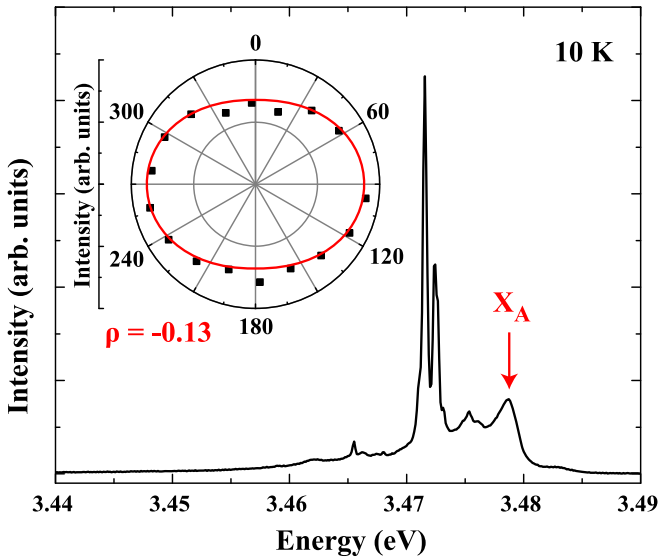

Figure 7. Photoluminescence spectrum of nanowire NW2 at 10 K. Inset: θ-dependence of the X_A emission intensity (symbols). The solid line shows the result of a fit using equation (1), which yields $\rho = -0.13$.

For all the nanowires investigated, the deviation of ρ from -1 is larger for the X_A than for the (D^0, X_A) transition. The same is true for the free and donor-bound B excitons: ρ ranges between -0.39 and -0.15 for the (D^0, X_B) line, whereas a value of 0.52 has been recorded for the X_B emission from the one nanowire in which this transition could be resolved (cf figure 6). We recall that for a freestanding GaN nanowire, one would expect the free B exciton emission to be nearly isotropic with $\rho = -0.08$ [42]. It is therefore clear that the deviation of the value of ρ from -1 for the X_A and (D^0, X_A) transitions can be attributed neither to a spectral overlap with lines related to the B exciton, nor to the deviation from the condition $\boldsymbol{k} \perp c$, nor a mixing between A and B valence bands introduced by the donor potential.

The observation of both (D^0, X_A) and X_A transitions for light polarized parallel to the c axis could arise from the fact that our dispersed nanowires are strained (figure 4). Whereas biaxial strain in the (0001) plane does not modify the selection rules for the X_A state, the X_A transition with $\boldsymbol{E} \parallel \boldsymbol{c}$ becomes allowed in the presence of strain components that lower the crystal symmetry [43, 44]. Indeed, an X_A line with $\boldsymbol{E} \parallel \boldsymbol{c}$ has been observed for nonpolar and semi-polar GaN layers grown on lattice-mismatched substrates [44–46]. However, while strain can alter the selection rules, it cannot account for our experimental findings alone. First, the largest difference between the energy of the X_A transition in the ensemble and the dispersed nanowires is 2 meV (figure 4). Using the results of [43] and [47], we find that the magnitude of this strain is too small to be accompanied by changes in the selection rules as drastic as those displayed in figures 6 and 7. Second, strain cannot explain why donor-bound A and B excitons do not show the same ρ as their corresponding free exciton states.

In the following, we investigate the possibility that the combination of strain with the antenna effect can explain our findings. First, we consider the case of GaN nanowires with $\phi \ll \lambda$, the polarization anisotropy of which can be written as [1]:

$$\frac{I^{\parallel}}{I^{\perp}} = \left(\frac{\epsilon + 1}{2}\right)^2 \tag{3}$$

with the dielectric constant ϵ. For wurtzite GaN, the dielectric constants for light polarized perpendicular and parallel to the nanowire axis ($\epsilon^{\perp}$ and $\epsilon^{\parallel}$, respectively) are different. Furthermore, excitons in wurtzite GaN are anisotropic emitters with different oscillator strengths perpendicular and parallel to the c-axis ($f^{\perp}$ and $f^{\parallel}$, respectively). When accounting for these facts, equation (3) reads:

$$\frac{I^{\parallel}}{I^{\perp}} = \left(\frac{\epsilon^{\perp} + 1}{2}\right)^2 \frac{f^{\parallel}}{f^{\perp}}. \tag{4}$$

As already discussed above, an anisotropic strain results in a nonzero value of $f^{\parallel}$ for the X_A transition. Using Equation (4) with $\epsilon^{\perp} = 9.4$, the X_A transition exhibits values of ρ larger than zero for $f^{\parallel}/f^{\perp} > 0.037$. For the bulk, such a small value for $f^{\parallel}/f^{\perp}$ would not result in a significant change of the purely perpendicular polarization of the emission, but due to the antenna effect, it results in an isotropic emission for thin nanowires.

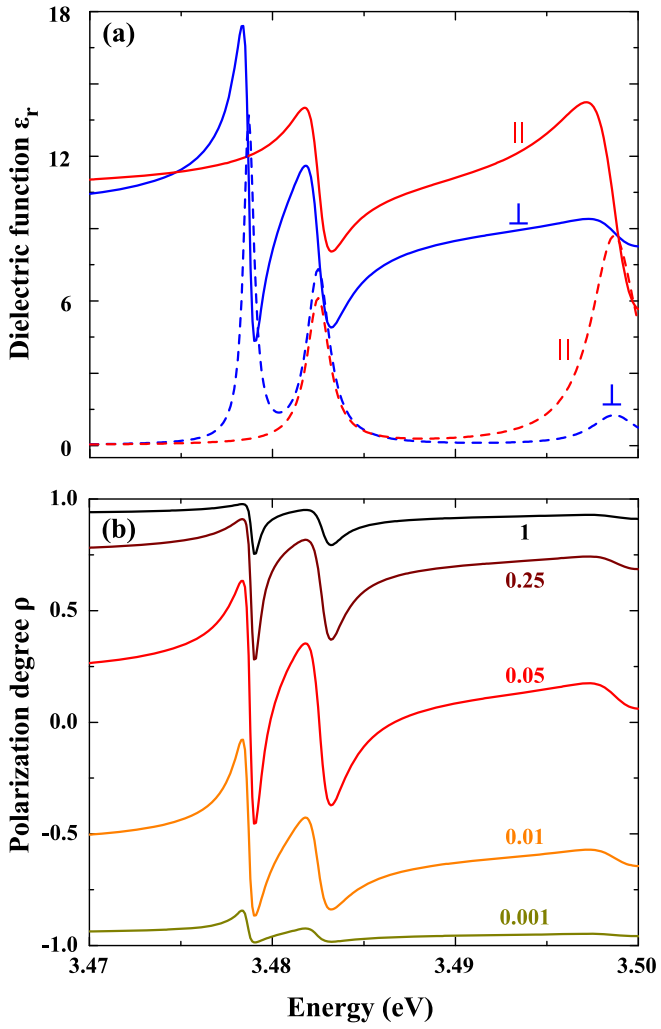

Figure 8. (a) Real (solid lines) and imaginary parts (dashed lines) of the dielectric function of strain-free GaN for light polarized perpendicular and parallel to the nanowire axis (blue and red, respectively), using the parameters in table 1. (b) Energy dependence of the polarization degree of an emitter located in a cylindrical GaN nanowire in the quasi-static case computed using equation (4) and accounting solely for the variation of the real part of ϵ_r due to the A, B, and C exciton resonances. The values for $f^{\parallel}/f^{\perp}$ are indicated in the figure.

Consequently, due the combination of strain with the antenna effect, excitonic transitions in GaN nanowires can exhibit energies similar to that of the bulk together with quite distinct polarization anisotropies.

Moreover, $\epsilon^{\parallel}$ and $\epsilon^{\perp}$ show strong variations as a function of the photon energy E due to the A, B, and C exciton resonances close to the band edge. Neglecting spatial dispersion, the dielectric function ϵ_r may be written as

$$\epsilon_r^j = \epsilon_b^j + \sum_{n=A,B,C} \frac{f_n^j}{E_n^2 - E^2 - i\gamma_n E}, \tag{5}$$

where the superscript j stands for $\perp$ or $\parallel$, f_n and γ_n are the oscillator strength and the homogeneous broadening of the free n exciton, and ϵ_b^j is the background dielectric constant (relative permittivity) with $\epsilon_b^{\perp} = 9.4$ and $\epsilon_b^{\parallel} = 10.2$ (see [48]). We assume that the transverse exciton energies are those measured for the X_A, X_B and X_C transitions on the as-grown nanowire ensemble (cf figure 2).

Figure 8(a) shows $\epsilon_r^{\perp}$ and $\epsilon_r^{\parallel}$ for bulk, strain-free GaN between 3.47 and 3.50 eV. The values for $f_n^{\perp}$, $f_n^{\parallel}$ and γ_n have been deduced from [49] and [42] and are compiled in table 1. Combining equations (4) and (5) and considering only the real part of ϵ_r, it becomes clear that an emitter with a given set of ($f^{\parallel}$, $f^{\perp}$) exhibits a strong spectral dependence of ρ in the near band-edge region. For instance, for an emitter with $f^{\parallel}/f^{\perp} = 0.05$, ρ varies between −0.46 and 0.64 in the 3.47–3.50 eV range as displayed in figure 8(b). In other words, although the X_A and (D^0, X_A) transitions possess the same value for $f^{\parallel}/f^{\perp}$, the values of ϵ_r at the corresponding energies are

Table 1. Parameters used in figure 8(a) for the contribution of A, B, and C excitons to the dielectric function of strain-free GaN for light polarized parallel ($\parallel$) and perpendicular ($\perp$) to the nanowire axis.

	A	B	C
E_n (eV)	3.4785	3.4825	3.4987
γ_n (meV)	0.7	1.5	3.1
$f_n^{\perp}$ (meV^2)	32700	37600	13500
$f_n^{\parallel}$ (meV^2)	0	32000	94300

different. Consequently, the polarization anisotropy of these two transitions is not equal in agreement with the experimental results displayed in figure 6.

Equation (4) only applies to the quasi-static case, i.e., for $\phi/\lambda \ll 1$. With $\phi/\lambda \approx 0.14$, the nanowires under investigation have sub-wavelength diameter and still do not support any guided modes. However, they do not correspond to the quasi-static limit either, and we examine in the following second step of our analysis whether or not our above conclusions also hold in this case. Note that polarization anisotropy related to the dielectric contrast between the nanowire and its environment is expected even for $\phi/\lambda \geqslant 1$, i.e., when the nanowires are thick enough to support several guided modes [2, 3, 5].

In what follows, we apply the model developed by Ruppin [50] for calculating the extinction of light by cylindrical nanowires with a diameter smaller or on the order of the wavelength. This model is applicable to media with complex ϵ_r, which is important when treating the polarization anisotropy of GaN nanowires near the band-edge (cf figure 8(a)). Furthermore, this model has been successfully used to describe the polarization anisotropy of both CdSe and GaAs nanowires with sub-wavelength diameter [51, 52].

Figure 9(a) shows the spectral dependence of ρ computed within the frame of this model for an emitter with $f^{\parallel} = f^{\perp}$ in a nanowire with $40 < \phi < 60$ nm and a constant $\epsilon_r^i = \epsilon_b^i$. When ϕ is increased from 30 to 50 nm, ρ decreases as a result of the finite diameter of the nanowire which causes the quasi-static approximation to break down [5]. For larger nanowire diameters, ρ starts to oscillate due to the progressive support of guided modes [3, 53]. Spontaneously formed GaN nanowires grown by molecular beam epitaxy, such as the ensemble investigated in the course of this work, invariably exhibit a broad diameter distribution (see figure 1 and [54]). In the present case, this distribution peaks at 50 nm but has a full width of 30 nm. This large variation in diameter explains the scatter of the values of ρ measured for different nanowires as shown in figure 6, and also reported in [4] and [6]. However, when neglecting the contribution of excitons to ϵ_r, ρ for a given ϕ and a given set of $(f^{\parallel}, f^{\perp})$ remains virtually constant between 3.47 and 3.50 eV. In other words, when $\epsilon_r^i = \epsilon_b^i$, the X_A and (D^0, X_A) transitions of a given nanowire should exhibit the same polarization degree. In contrast, when the contribution of excitons to $\epsilon_r^{\perp}$ and $\epsilon_r^{\parallel}$ is taken into account, ρ depends strongly on both the energy and the nanowire diameter as shown in figure 9(b). For instance, for a nanowire with $\phi = 70$ nm and for $f^{\parallel} = f^{\perp}$, transitions at 3.474 and 3.482 eV exhibit a value of ρ equal to 0.66 and −0.39, respectively. The strong variations of the real and imaginary parts of ϵ_r at the exciton resonances thus manifest themselves by the different values of ρ measured for the bound and free exciton transitions.

A truly quantitative comparison of the calculated polarization degree with our experimental results summarized in figure 6 is not straightforward, since our analysis is based on several assumptions which only crudely approximate reality. In particular, the shape of spontaneously formed GaN nanowires may differ significantly from that of the cylinder assumed for our calculations, primarily due to the coalescence of adjacent nanowires during their growth [54]. Furthermore, our nanowires are not only surrounded by air, but have been dispersed on a TiAu mask, which leads to a detectable change of the polarization compared to that of the free-standing nanowire [5]. In reality, we are thus dealing with irregularly shaped nanowires with a dielectrically inhomogeneous environment, and these two facts make any quantitative comparison computationally challenging. With regard to these limitations, the changes of ρ with energy and nanowire diameter as predicted by our simple model above are in very satisfactory qualitative agreement with experiment.

The real and imaginary parts of ϵ_r being almost constant between 3.45 and 3.47 eV, the previous discussion cannot explain the counter-polarization observed between the (D^0, X_A) and the UX_1 bands. Therefore, the excitons bound to the defect giving rise to the (D^0, X_A) and the UX_1 transitions show different selection rules. Now, the defect related to the UX_1 transition is likely to be related to the surface [13, 14, 17, 26, 27]. As pointed out in [13], the selection rules for surface excitons may deviate from what is expected for the X_A. In addition, for thin nanowires, a slight deviation of the selection rules is accompanied by a strong change in the polarization degree (see equation (4) and figure 8(b)). The statistical distribution in the distance between the surface and this

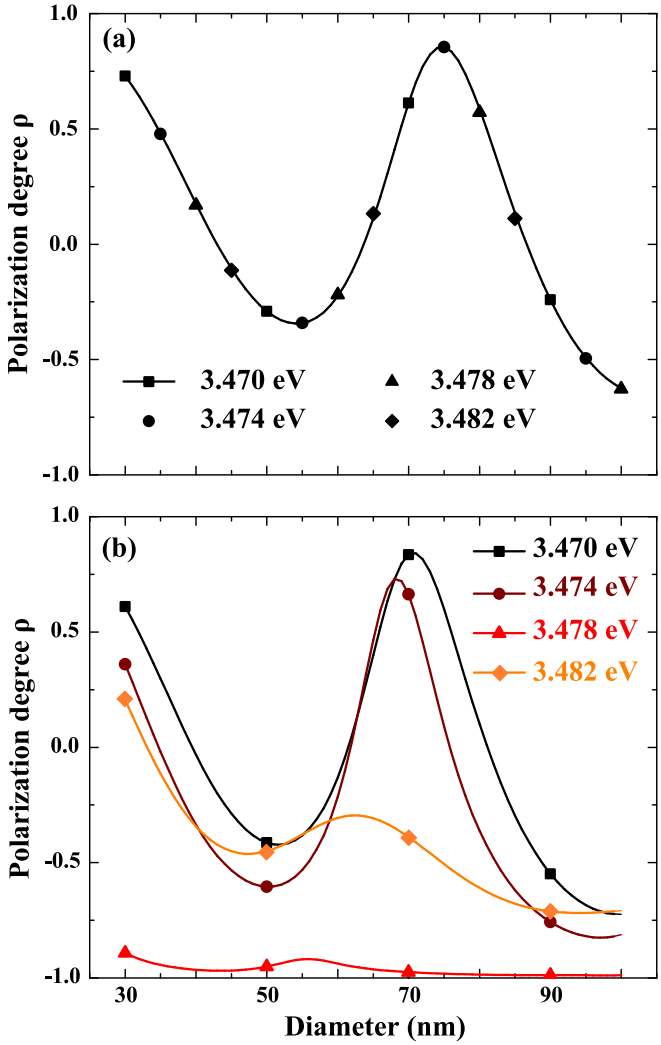

Figure 9. Polarization degree as a function of the nanowire diameter for an emitter with $f^{\parallel} = f^{\perp}$ and with an emission energy equal to 3.470 (squares), 3.474 (circles), 3.478(triangles), and 3.482 eV (diamonds). In (a), $\epsilon_r^i = \epsilon_b^i$, and the computed polarization degrees overlap almost perfectly. In (b), the exciton resonances are taken into account, and the polarization degree depends strongly on the emission energy.

point defect thus results in a distribution in the energy of the UX_1 transitions (figures 3 and 6) and in slight variations in the selection rules. The latter translate into a large scattering of values for the polarization degree of the UX_1 lines, in agreement with the observation made in figure 6.

5. Summary and conclusion

We have studied the polarization of excitonic transitions of single, dispersed GaN nanowires. The strain introduced during the nanowire dispersion leads to a mixing of the A and B bands, and thus transfers oscillator strength to the X_A transition polarized parallel to [0001] which is forbidden in strain-free GaN. In addition, the sub-wavelength diameter of our nanowires gives rise to a pronounced antenna effect that amplifies this apparent oscillator strength parallel to [0001] by more than an order of magnitude. As a result, the polarization of the X_A emission depends sensitively on the particular strain state and diameter of a given nanowire, and may even appear to be isotropic. The strong variations of the dielectric function in the near band-edge region furthermore lead to a different polarization anisotropy for donor-bound excitons and the free exciton states they are derived from. Consequently, the combination of strain, surface-induced wavefunction distortion and the dielectric contrast between the nanowire and its environment result in a complex polarization anisotropy of excitonic transitions in dispersed nanowires. Great care must be taken when comparing the intensity of bound and free exciton transitions to extract, for example, information on the radiative and nonradiative lifetimes of the corresponding states as it is possible in a straightforward way for bulk GaN [36].

Acknowledgments

The authors thank Carsten Pfüller, Jonas Lähnemann, and Anne-Kathrin Bluhm for carrying out the secondary electron microscopy. They are furthermore indebted to Manfred Ramsteiner for a critical reading of the manuscript, and to Lutz Geelhaar, Holger Grahn, and Henning Riechert for continuous encouragement and support. Partial funding by the Deutsche Forschungsgemeinschaft within SFB 951 is gratefully acknowledged.

References

[1] Wang J, Gudiksen M S, Duan X, Cui Y and Lieber C M 2001 *Science* **293** 1455–7
[2] Balzer F, Bordo V, Simonsen A and Rubahn H G 2003 *Phys. Rev.* B **67** 115408
[3] Ruda H E and Shik A 2006 *J. Appl. Phys.* **100** 024314
[4] Chen H Y, Yang Y C, Lin H W, Chang S C and Gwo S 2008 *Opt. Express* **16** 13465–75
[5] Zhang J, Lutich A A, Rodríguez-Fernández J, Susha A S, Rogach A L, Jäckel F and Feldmann J 2010 *Phys. Rev.* B **82** 155301
[6] Rigutti L, Tchernycheva M, de Luna Bugallo A, Jacopin G, Julien F H, Furtmayr F, Stutzmann M, Eickhoff M, Songmuang R and Fortuna F 2010 *Phys. Rev.* B **81** 045411
[7] Grzela G, Paniagua-Domínguez R, Barten T, Fontana Y, Sánchez-Gil J A and Gómez Rivas J 2012 *Nano Lett.* **12** 5481–6
[8] Fontana Y, Corfdir P, Van Hattem B, Russo-Averchi E, Heiss M, Sonderegger S, Magen C, Arbiol J, Phillips R T and Fontcuberta i Morral A 2014 *Phys. Rev.* B **90** 075307
[9] Mishra A *et al* 2007 *Appl. Phys. Lett.* **91** 263104
[10] Spirkoska D, Efros A, Lambrecht W R L, Cheiwchanchamnangij T, Fontcuberta i Morral A and Abstreiter G 2012 *Phys. Rev.* B **85** 045309
[11] Efros A L and Lambrecht W R L 2014 *Phys. Rev.* B **89** 035304
[12] Schlager J B, Sanford N A, Bertness K A, Barker J M, Roshko A and Blanchard P T 2006 *Appl. Phys. Lett.* **88** 213106
[13] Sam-Giao D, Mata R, Tourbot G, Renard J, Wysmołek A, Daudin B and Gayral B 2013 *J. Appl. Phys.* **113** 043102
[14] Calleja E, Sánchez-García M, Sánchez F, Calle F, Naranjo F, Muñoz E, Jahn U and Ploog K H 2000 *Phys. Rev.* B **62** 16826–34
[15] Kaganer V M, Jenichen B, Brandt O, Fernández-Garrido S, Dogan P, Geelhaar L and Riechert H 2012 *Phys. Rev.* B **86** 115325
[16] Robins L H, Bertness K A, Barker J M, Sanford N A and Schlager J B 2007 *J. Appl. Phys.* **101** 113505
[17] Corfdir P, Lefebvre P, Ristić J, Valvin P, Calleja E, Trampert A, Ganière J D and Deveaud-Plédran B 2009 *J. Appl. Phys.* **105** 013113
[18] Brandt O, Pfüller C, Chèze C, Geelhaar L and Riechert H 2010 *Phys. Rev.* B **81** 45302
[19] Corfdir P, Zettler J K, Hauswald C, Fernández-Garrido S, Brandt O and Lefebvre P 2014 *Phys. Rev.* B **90** 205301
[20] Fernández-Garrido S, Grandal J, Calleja E, Sánchez-García M A and López-Romero D 2009 *J. Appl. Phys.* **106** 126102
[21] Geelhaar L *et al* 2011 *IEEE J. Sel. Top. Quantum Electron.* **17** 878–88
[22] Consonni V 2013 *Phys. Status Solidi (RRL)* **7** 699–712
[23] Heying B, Averbeck R, Chen L F, Haus E, Riechert H and Speck J S 2000 *J. Appl. Phys.* **88** 1855
[24] Corfdir P, Hauswald C, Zettler J K, Flissikowski T, Lähnemann J, Fernández-Garrido S, Geelhaar L, Grahn H T and Brandt O 2014 *Phys. Rev.* B **90** 195309
[25] Stan G, Krylyuk S, Davydov A V and Cook R F 2012 *J. Mater. Res.* **27** 562–70
[26] Furtmayr F, Vielemeyer M, Stutzmann M, Laufer A, Meyer B K and Eickhoff M 2008 *J. Appl. Phys.* **104** 74309
[27] Lefebvre P, Fernández-Garrido S, Grandal J, Ristić J, Sánchez-García M A and Calleja E 2011 *Appl. Phys. Lett.* **98** 083104
[28] Chisholm J A and Bristowe P D 2000 *Appl. Phys. Lett.* **77** 534
[29] Paskov P, Paskova T, Holtz P O and Monemar B 2004 *Phys. Rev.* B **70** 83–86
[30] Toyozawa Y 1959 *Prog. Theor. Phys. Suppl.* **12** 111
[31] Sell D D, Stokowski S E, Dingle R and DiLorenzo J V 1973 *Phys. Rev.* B **7** 4568–86
[32] Hauswald C *et al* 2014 *Phys. Rev.* B **90** 165304
[33] Weisbuch C and Ulbrich R G 1979 *J. Lumin.* **1819** 27–31
[34] Schultheis L and Tu C W 1985 *Phys. Rev.* B **32** 6978–81
[35] Steiner T, Thewalt M L W, Koteles E S and Salerno J P 1986 *Phys. Rev.* B **34** 1006–13
[36] Leroux M, Grandjean N, Beaumont B, Nataf G, Semond F, Massies J and Gibart P 1999 *J. Appl. Phys.* **86** 3721
[37] Corfdir P and Lefebvre P 2012 *J. Appl. Phys.* **112** 106104
[38] Schlager J B, Bertness K A, Blanchard P T, Robins L H, Roshko A and Sanford N A 2008 *J. Appl. Phys.* **103** 124309
[39] Dietrich C P, Lange M, Klüpfel F J, von Wenckstern H, Schmidt-Grund R and Grundmann M 2011 *Appl. Phys. Lett.* **98** 031105
[40] Park J B, Hong W K, Bae T S, Sohn J I, Cha S, Kim J M, Yoon J and Lee T 2013 *Nanotechnology* **24** 455703
[41] Fu X *et al* 2014 *Adv. Mater.* **26** 2572–9
[42] Misra P, Brandt O, Grahn H T, Teisseyre H, Siekacz M, Skierbiszewski C and Łucznik B 2007 *Appl. Phys. Lett* **91** 141903
[43] Gil B and Alemu A 1997 *Phys. Rev.* B **56** 12446–53
[44] Ghosh S, Waltereit P, Brandt O, Grahn H and Ploog K 2002 *Phys. Rev.* B **65** 075202
[45] Paskov P, Schifano R, Monemar B, Paskova T, Figge S and Hommel D 2005 *J. Appl. Phys.* **98** 093519
[46] Gühne T, Bougrioua Z, Laügt S, Nemoz M, Vennéguès P, Vinter B and Leroux M 2008 *Phys. Rev.* B **77** 075308
[47] Jacopin G *et al* 2012 *Nanotechnology* **23** 325701
[48] Azuhata T, Sota T, Suzuki K and Nakamura S 1995 *J. Phys.: Condens. Matter* **7** L129
[49] Stępniewski R, Korona K P, Wysmołek A, Baranowski J M, Pakuła K, Potemski M, Martinez G, Grzegory I and Porowski S 1997 *Phys. Rev.* B **56** 15151–6
[50] Ruppin R 2002 *Opt. Commun.* **211** 335–40
[51] Giblin J, Protasenko V and Kuno M 2009 *ACS Nano* **3** 1979–87
[52] Ramsteiner M, Brandt O, Kusch P, Breuer S, Reich S and Geelhaar L 2013 *Appl. Phys. Lett.* **103** 043121
[53] Li H Y, Rühle S, Khedoe R, Koenderink A F and Vanmaekelbergh D 2009 *Nano Lett.* **9** 3515–20
[54] Brandt O, Fernández-Garrido S, Zettler J K, Luna E, Jahn U, Chèze C and Kaganer V M 2014 *Cryst. Growth Des.* **14** 2246–53